



2 W power source based on air–hydrogen polymer electrolyte membrane fuel cells and water–aluminum hydrogen micro-generator

Eugene Shkolnikov, Mikhail Vlaskin*, Alexey Iljukhin, Andrey Zhuk, Alexander Sheindlin

The Joint Institute for High Temperatures, Ijorskaya St. 13/19, 125412 Moscow, Russia

ARTICLE INFO

Article history:

Received 21 March 2008

Received in revised form 27 August 2008

Accepted 10 September 2008

Available online 26 September 2008

Keywords:

PEM FC

Portable power source

Water–aluminum hydrogen

micro-generator

Free-breathing

Limited volume conditions

Joint testing

ABSTRACT

The article presents an attempt to design the 2 W power source (PS) based on air–hydrogen fuel cells (FCs) and water–aluminum micro-generator as a hydrogen supply (WAHMG). Experiments concern FC's breathing in compact arrangement and combined performance of FC + WAHMG. It turned out to be necessary to build a fan into FC stack provided the rotation speed of fan depends on the FC current. The highest power density of FC at optimal speed of air blowing was 101 mW cm^{-2} . Electrical energy produced by FC was about 1.2–1.8 Wh per gram of Al in micro-generator. This value depends on the total yield of hydrogen in WAHMG and hydrogen losses due to purges.

© 2008 Elsevier B.V. All rights reserved.

1. Introduction

Impetuous growth of the electronics market provides the high demand for accumulators with higher energy density. This circumstance has increased interest to small-scale fuel cells (FCs) as alternative sources of the electric power. This is the reason why a great number of the leading companies and research institutes, such as Angstrom, DoCoMo, Hitachi Maxell, Canon, Protonex, DCP China, SAIT Korea, etc. [1,2], develop the FCs for portable electronics today. Basic problems are fuel accumulation and optimum FC design, cost and durability. Today, hydrogen and methanol are mainly used as fuel for developed prototypes of portable FCs [3]. There are three applicable ways of hydrogen production on-board, all are based on displacement of hydrogen from water by active redoxing chemicals; interaction of magnesium and magnesium-based alloys with water [4,5]; interaction of activated aluminum and its alloys with water [6–10]; and hydrogen from sodium boranes in the presence of water and corresponding catalysts [11–17].

The present article gives the description of 2 W power source (PS) prototype based on solid polymer electrolyte membrane fuel

cells (PEM FCs) and WAHMG used as a hydrogen source. Hydrogen is produced from water reacting with aluminum. Alkalis or other additives for water are not used.

So, an object of our work was to develop a PS and also study various operating modes of its components and the PS as a whole.

A device to be developed should meet the following requirements:

- (1) the PS should be safe and easy to use;
- (2) the PS should be compact;
- (3) hydrogen production in WAHMG should be in accordance with consumption in FC [18];
- (4) aluminum and water for WAHMG should be in a cheap and easy-replaceable cartridge [19];
- (5) stacks of FCs should be two-cell for possibility to operate in “free-breathing” mode [20].

2. PS description

2.1. PS design

The 2 W PS (Fig. 1) has been developed as cellular phone charger for use in case when charge from electricity network is impossible. With small modification, such PS can be used for any portable device having load characteristics similar to cellular phone accumulators. The described type of PS includes a hydrogen micro-

* Corresponding author. Tel.: +7 495 4859411; fax: +7 495 4859411.

E-mail addresses: 2shkolnikov@ined.ras.ru (E. Shkolnikov), vlaskin@inbox.ru (M. Vlaskin), ilyukhin@ihed.ras.ru (A. Iljukhin), zhuk@ihed.ras.ru (A. Zhuk).



Fig. 1. 2 W PS for cellular phone accumulators charging.

generator, two two-cell free-breathing FC stacks, chip controller with DC/DC converter/voltage stabilizer and an electromagnetic valve.

The hydrogen generator consists of replaceable cartridge (Fig. 2) located in a hermetical case. The cartridge consists of two parts: a water container and an activated aluminum compartment. Water is in a special porous material. Both parts are divided by a membrane with adjusted porous structure. There are water-holding separators for catching liquid water, which goes with hydrogen from the cartridge to FCs. Separators are located near the WAHMG output. To charge a mobile phone, user should only insert the cartridge into PS's case and attach the phone to power cord of PS.

When starting the WAHMG, a pressure in WAHMG + FC system quickly increases. A large excess pressure can damage the FC; therefore, a safety electromagnetic valve is used to regulate pressure. The valve provides a gas purge when the pre-defined pressure value is exceeded. Valve also does the initial purge in the beginning of WAHMG operation. The initial purge is intended to remove air, which originally fills the system.

The electromagnetic valve is controlled by the controller. The basic function of DC/DC converter is transforming the FC voltage into a predetermined output voltage. All said components are united into a single case of a flat rectangular shape (Fig. 1). Characteristics of the micro-PS are shown in Table 1.

2.2. Free-breathing FC design

FC stack contains three-layer membrane electrode assemblies (MEAs) and gas-diffusion layers (of 200 μm thick) available from

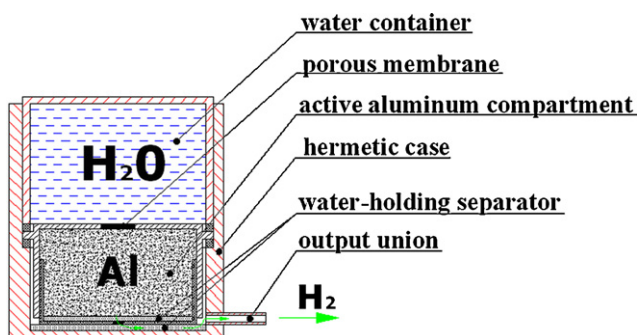


Fig. 2. WAHMG structure.

Table 1
Technical parameters of the 2 W micro-PS.

Specification	Measurement unit	Value
Rated power	W	2
Maximum power	W	3
Operating voltage	V	4.6
Operating current	mA	440
Energy density of water–aluminum cartridge	$\text{Wh g}^{-1}(\text{Al})$	1.2–1.8
Average cartridge start time	S	10
Operating temperature	$^{\circ}\text{C}$	5–45
Overall dimensions of PS	$\text{cm} \times \text{cm} \times \text{cm}$	$6.5 \times 13.6 \times 2.5$
Mass	g	280

Golden Energy Fuel Cell (GEFC, China [21]). A proton-conductive membrane has a thickness of 25 μm .

Fig. 3 is a structural diagram of a two-cell stack. The two-cell stack consists of two air–hydrogen PEM FCs with common hydrogen chamber. The hydrogen chamber is a polymer frame having a U-shaped hydrogen flow field. A thickness of the hydrogen frame is 2.5 mm, an overall size is 58 mm \times 24 mm. Hydrogen is supplied into the chamber by means of the unions of 1.6 mm diameter, which are glued into the frame.

Plates of 1.2-mm thick with slits for air supplying to cathodes perform mechanical compression and current collection from the cathodes. An open-to-closed portion ratio of the active cathode surface is 3:2. The material of these plates is titanium. The plates are compressed by means of screws. An overall size of external titanic plates and external gas-diffusion layers is 58 mm \times 24 mm. This size is defined by both the general PS design and the term of mechanical compression, which is necessary to reduce the contact losses. The length-to-width ratio is larger, the distance from any point of active surface to nearest screw is smaller, so the mechanical pressure in this point is larger. Due to the choice of such FC shape, thickness and material of external plates, we were succeeded in refusing massive end plates. Plates of 0.8-mm thick with slits for hydrogen supplying to an anode perform current collection from the anodes. An open-to-closed portion ratio of the active anode surface is 1:1. An overall size of internal plates and gas-diffusion layers is 52 mm \times 12 mm. The material of internal plates is titanium too.

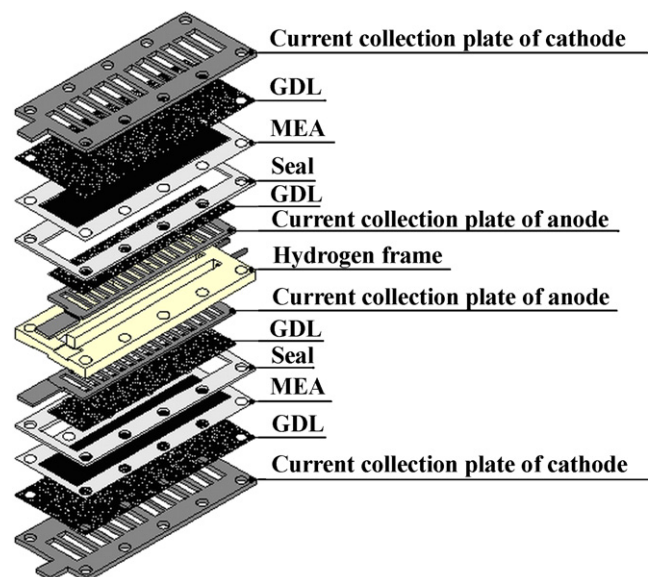


Fig. 3. Structural diagram of a two-cell free-breathing FC stack.

An active cell surface area is 6.24 cm^2 , i.e. a stack consisting of two FCs has an active surface of 12.5 cm^2 while the PS consisting of two two-cell stacks has an active surface of 25 cm^2 . A stack thickness from one external titanite plate to another in the compressed state is 6.8 mm . A distance from screw heads to nuts is 11.4 mm . A weight of such stack is 25 g . All cells are connected in series for output voltage increase.

3. Experimental

3.1. FC test procedure

Experiments were carried out on single cell of the two-cell stack to avoid influence of one element upon another when they are connected in series. Hydrogen was supplied to the FC from an electrolyzer at a constant pressure of 1.5 atm . Stationary values of power density at constant external load and current–voltage curves were chosen to compare FC operation under different ambient conditions.

We distinguish three current density ranges: small current density, $<200\text{ mA cm}^{-2}$; medium current density, $200\text{--}500\text{ mA cm}^{-2}$; and large current density, $>500\text{ mA cm}^{-2}$. When developing the PS prototype, we aspired to obtain maximum values of power density at rather high voltages on the FC to provide an acceptable efficiency ($>40\%$) of the FC which, as everybody knows, is directly proportional to its voltage [22]. The large current density region, $>500\text{ mA cm}^{-2}$, does not satisfy this condition because our FC in this case operates in the region of great diffusion losses, so the FC efficiency is accordingly low, smaller than 20% (Fig. 4). Therefore, all experiments were carried out within the region where the current densities were $<250\text{ mA cm}^{-2}$.

The assumed FC operating mode in PS represents periodic starts for a time up to 1 h and “a rest” between these starts. To simulate this mode, each measurement cycle was continued not less than 60 min . During this time, the cell was achieving its stationary power value. For all this time, the FC current and voltage values were measured continuously and served to trace a power density change in time. Fig. 5 shows the power density in long-term free-breathing mode experiment for MEAs after different treatment. Curve (1) is for MEA “as delivered” (without any preliminary treatment) within the small current density region; curves (2) and (3) are for MEAs

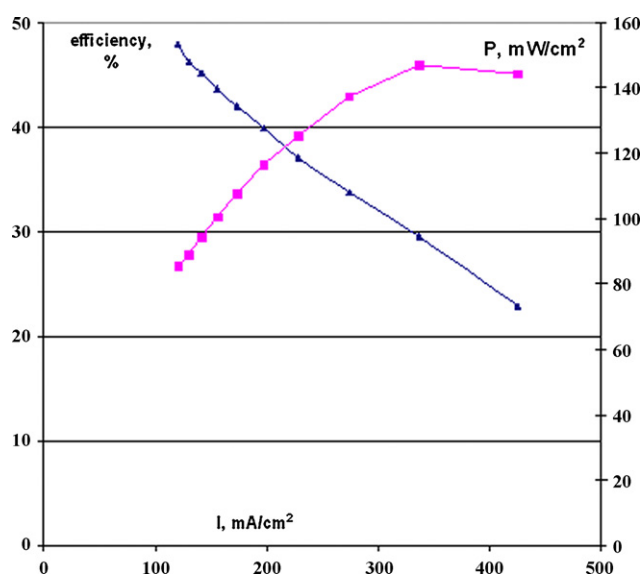


Fig. 4. Typical efficiency and power density values for free-breathing FCs.

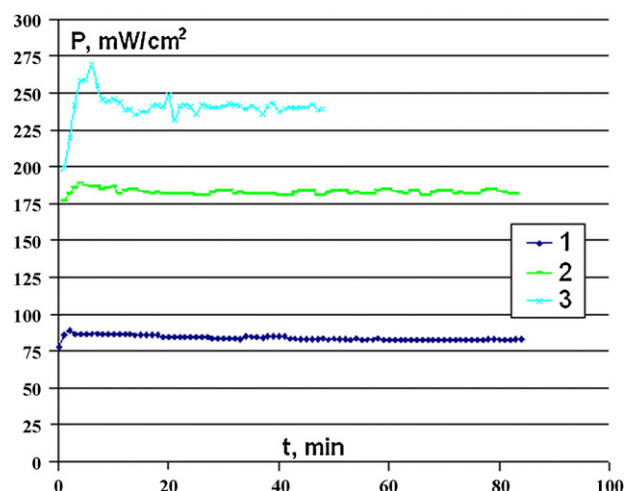


Fig. 5. Typical curves describing the FC power density change in time during long-term experiment for MEAs having different water contents. Curve (1) is power density change in time of FC with MEA as delivered in small current density region; curves (2) and (3) are power density changes of the FC with MEA treated according to a special technique in the sulfuric acid solution within the small and medium current density regions, respectively.

treated according to a special technique in the sulfuric acid solution within the small and medium current density regions, respectively. In the presented case, curves (2) and (3) only show a level of characteristics achieved in our FCs after special treatment of MEAs and have no relation to results below.

In the end of each experiment, there was measurement of current–voltage characteristic whose graphs will be considered in Section 4. The FC current–voltage characteristics were determined in the direction of current density increase. Points on the current–voltage curves were read at a delay of 10 s . After that experiment was finished and the cell had “a rest” for at least an hour.

Experiments on FCs was carried out in three modes (cathodes were oriented vertically in all modes):

1. “Natural Convection in Unlimited Volume (NCUV)”–Cathodes are under unlimited volume conditions, i.e. have direct access to surrounding air, without the forced air blow.
2. “Natural Convection in the Cathode Gap (NCCG)”–When cathodes are covered by a plate, with the gap of 2.5 mm between cathode and plate to supply air. Consumption of air by the cell still occurs due to natural convection.
3. “Forced Convection in the Cathode Gap (FCCG)”–Differs from the previous in that in this case air is fed to the cathodes by forced convection in addition to natural due to fan blowing in cathode gap.

Further, the FC electric characteristics were determined on the same FC within the same current region depending on the speed of cathode purging. The two-cell stack was located in the special case during the experiments. The case has been intended to provide passage of all air blown into the case directly under the cathode surface in the gap of 2.5 mm in height, 52 mm in length and 12 mm wide (Fig. 6). Air was fed into the case from hydrogen unions’ side, passed above cathode surface throughout its length and went out of the electric contacts side. The stack was arranged in a horizontal plane, wherein the face side of the studied cathode has been turned upwards. To provide quantitative check of the speed of cathode purging, environment air was supplied into the case by means of micro-compressor, which provided a higher pressure than

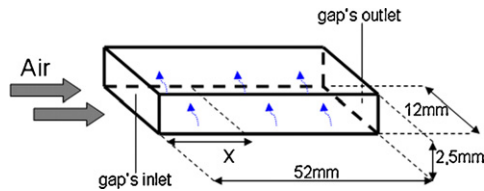


Fig. 6. Gap structure.

a fan at an inlet of the gas path. The pressure produced by fan was insufficient for effective purging the test air–gas system.

The supply rate was established by a throttling device and measured by means of a flow sensor. Air humidity and temperature were measured at the gap inlet and outlet. In each experiment the speed of cathode purging was maintained constant.

3.2. Joint WAHMG + FC test procedure

Conditions of separate tests of WAHMG and FC operating do not correspond to conditions of their joint operation because hydrogen consumption in the FC under conditions of separate tests occurs irrespective of its production in WAHMG.

The purpose of experiments described below was to determine the total electric energy produced per water–aluminum cartridge and to study basic functional system parameters (working pressures, hydrogen production and consumption rate, FC current–voltage characteristics) during operation of a charger model.

In experiments of the joint WAHMG + FC operation FC battery was directly connected to electronic load (without the DC/DC-converter), that allowed to determine a total voltage of two two-cell FC stacks in galvanostatic mode. A temperature of the WAHMG and a pressure in the gas path were determined by means of the laboratory plant shown in Fig. 7. The fixed quantity of an aluminum powder (from 0.5 g) together with water-conducting and water-catching membranes were located in a special compartment, and then in the WAHMG case the water and aluminum parts were got into contact with each other. When the WAHMG was started, production of hydrogen was fixed according to pressure increase in the system and to occurrence of a voltage at the FCs. To remove air from the system and achieve an open circuit voltage (OCV), a quantity of hydrogen was removed manually by means of faucet in the very beginning of experiment. Therefore, the first automatic purge of the gas path was simulated.

After FC voltage had been reached the OCV, the electronic load was started in the galvanostatic mode. If the pressure exceeded 2 atm during operation, the hydrogen system was purged to simulate following mechanical purges of the electromagnetic valve. The output of hydrogen in case of purges was measured by a volumetric method.

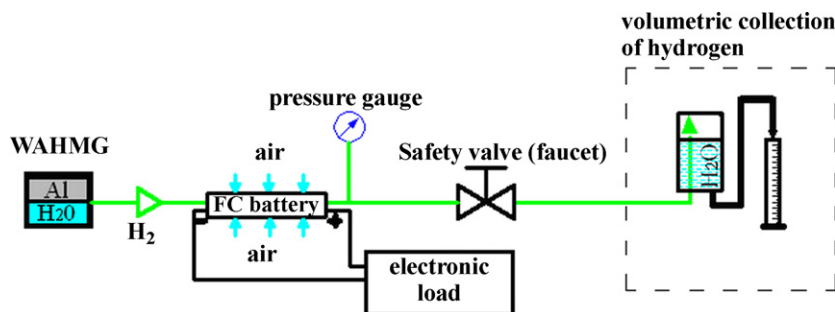


Fig. 7. Laboratory plant for joint WAHMG + FC tests.

Table 2

Stationary power densities of single FC for NCUV, NCCG and FCCG modes.

Mode	I (mA cm ⁻²)	P (mW cm ⁻²)
NCUV	135	83
NCCG	136	88
FCCG	149	97

4. Results and discussion

4.1. FC operation under limited volume conditions

Stationary power densities of single FC for NCUV, NCCG and FCCG modes are presented in Table 2. The temperature of air in experiments was 26 °C, and the relative humidity was 38%. The NCUV mode, when two-element stack is under unlimited volume conditions, is a basic mode for FC characteristics comparison in different conditions. It follows from Table 2 that transiting from the NCUV mode to the NCCG mode has positive effect within the small current density region. We are of the opinion that this effect is associated with some additional humidification of the initial MEA due to increasing of air humidity within a near-cathode space in the NCCG mode as compared to the NCUV mode. Thus, natural convection was still sufficient to support the corresponding stationary power density. This result is important for us, because the operating mode of two-element FC stacks in micro-PS body is the closest one to NCCG mode conditions. This result gives the basis to believe that there is no necessity to develop PSs with a great surface area for the open access of air to the FCs, and also confirms rationality of the chosen design of two-cell stacks.

Increase in the air blow due to creation of forced convection through the gap at the cathode by means of the fan has led to further increase in the stationary power density (approximately, up to 100 mW cm⁻²).

FC operation improvement in the FCCG mode has caused the urgency of carrying out the FC tests with various speeds of purging the gap at the cathode in order to determine an optimum purging speed and corresponding stationary power density.

The results of experiments with different speeds of cathode gap purging, including free-breathing regime, are shown in Fig. 8(a and b). The results of experiments are shown in the form of current–voltage curves and power curves. In those experiments FC was loaded to a 0.7 Ω. A temperature of ambient air supplied into the gap was $T_{in} = 26$ °C, and relative humidity RH_{in} was within an interval of 37–40%.

Stationary current and voltage values at such resistance on the current–voltage curves correspond to points having the fourth (from the left) value of the current density and encircled in Fig. 8(a). The same relates to the power curves (Fig. 8(b)).

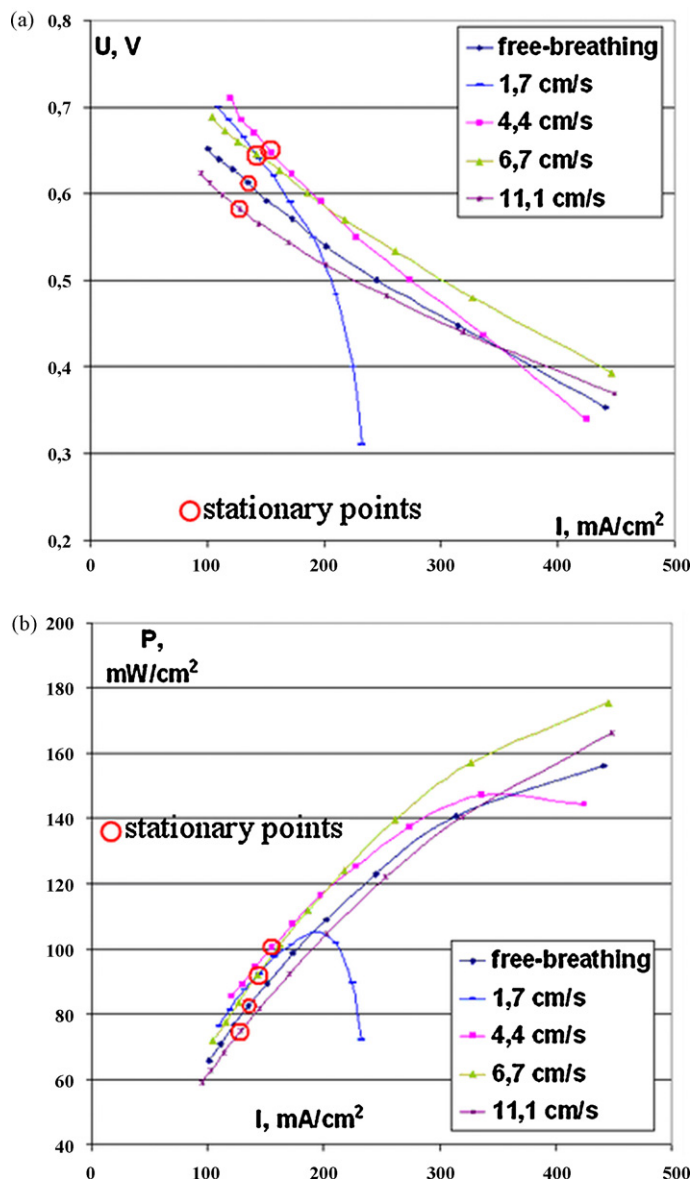


Fig. 8. Current–voltage curves (a) and power curves (b) associated therewith depending upon the speed of cathode gap purging as compared to the NCUV mode. An interval between points is 10 s.

Table 3 shows stationary values of the current density and power density depending on the speed of cathode gap purging as well as the temperature and relative humidity at the output of the gap (T_{out} and RH_{out}). It follows from the table that an optimum value of the speed is 4.4 cm s^{-1} within the small current density region considered by us. However this speed becomes obviously insufficient at transition to medium current values. It is seen from Fig. 8(a) that while the purging speed increases, current–voltage curves become more flat. It testifies to smaller diffusion losses in the FC at transition

Table 3

Stationary current and power density values depending on the rate of cathode gap purging and the humidity of supplied air, obtained in experiments.

$(dV_{\text{air}}/dt) (\text{cm s}^{-1})$	$T_{\text{in}} (^{\circ}\text{C})$	$\text{RH}_{\text{in}} (\%)$	$T_{\text{out}} (^{\circ}\text{C})$	$\text{RH}_{\text{out}} (\%)$	$I (\text{mA cm}^{-2})$	$P (\text{mW cm}^{-2})$
1.7	26		38	99	144	93
4.4	26		38	99	155	101
6.7	26	37–40	37	88	143	92
11.1	26		35	72	128	75

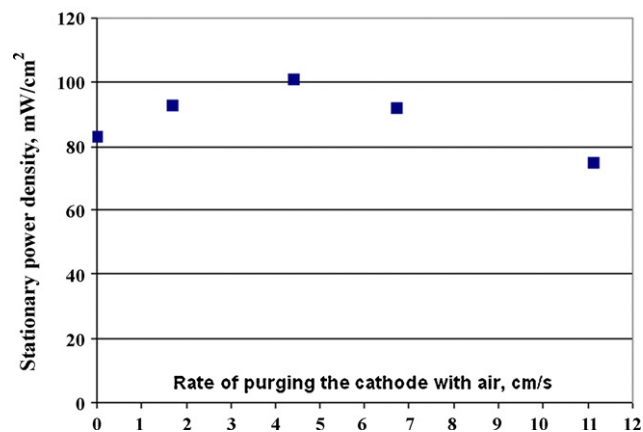


Fig. 9. Stationary power density values depending upon the speed of cathode gap purging. Comparison with stationary power density value in the BF mode.

to the medium current density region. In turn, there is a significant humidity loss from the gap at small current densities, because of that the cell in this region operates worse. On the contrary, we have significant diffusion losses within the medium current density region at small purging speeds. Besides, the cell operates noticeably better in the small current density region ($\sim 150 \text{ mA cm}^{-2}$) within the limited volume than in the NCUV mode because of humidifying air in the gap due to water evaporation from the cathode. It is possible to gain the benefit of up to several tens of mW cm^{-2} (Fig. 9, Fig. 8(a)) when the speed of cathode gap purging is optimal. From one hand, the optimum purging speed provides the sufficient air quantity in the gap at the cathode, and from the other hand, it maintains a high humidity of air in the gap, so it contributes to good humidifying of the surface of electrodes and the membrane itself.

The effect of clear dependency of the FC power upon the speed of purging its cathode without additional air humidification allows assumption that it would be expedient to mount a fan into our PS, while the rotation speed of said fan should depend upon current which in turn determines air consumption on the cathode.

4.2. Joint WAHMG + FC operation

Fig. 10 shows results of typical experiment for joint WAHMG + FC testing. The water–aluminum cartridge contained 0.9 g of Al and 7 ml of water, respectively. The battery of two two-cell free-breathing FC stacks connected in series was directly connected to the electronic load in the galvanostatic mode at a current of 1 A. The line (1) characterizes the total hydrogen consumption (30 ml min^{-1}) in the two-cell stacks calculated on the basis of the Faraday law. The hydrogen consumption rate is constant because the current determined by the electronic load was constant during experiment. The hydrogen production rate was calculated according to the equation:

$$\frac{dV}{dt} = V_0 \left(\frac{dP}{dt} \right) \left(\frac{1}{P_{\text{atm}}} \right) + k \times I \times n$$

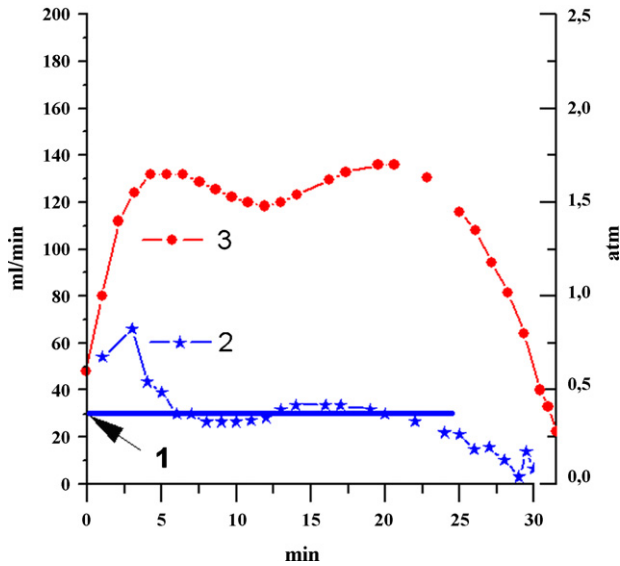


Fig. 10. System parameters (hydrogen consumption and production rates (1) and (2), system pressure (3)) during joint WAHMG + FC operation.

where dV/dt ($\text{cm}^3 \text{min}^{-1}$) is the hydrogen production rate, V_0 (cm^3) is the total volume of the gas system (WAHMG + hydrogen chambers of two-cell FC stacks + connection tubes), dP/dt (atm min^{-1}) is the pressure change rate, $P_{\text{atm}} = 1 \text{ atm}$, $k \approx 7.5$ ($\text{ml} (\text{min} \times \text{A})^{-1}$) is a volume of hydrogen consumed by one FC per time unit at 1 A, and n is the number of FCs. Fig. 10 shows that the system pressure grew (curve 3) when the hydrogen production rate (curve 2) was more than the hydrogen consumption rate (straight line 1), and vice versa.

As a result of oxidation of 0.9 g Al, the total output of hydrogen in the experiment was 913 ml (78% of the theoretical value). At the same time, the battery transformed 840 ml of hydrogen (70% of the theoretical value) into the electric power. 73 ml of hydrogen were lost as a result of purges of the gas system during experiment. The FC battery operated for approximately 30 min at an average voltage of 2.24 V (Fig. 11). Thus, the total electric energy produced per water–aluminum cartridge contained 0.9 g Al was 1.12 Wh. It corresponds to energy density of 1.25 Wh g^{-1} (Al). This value depends

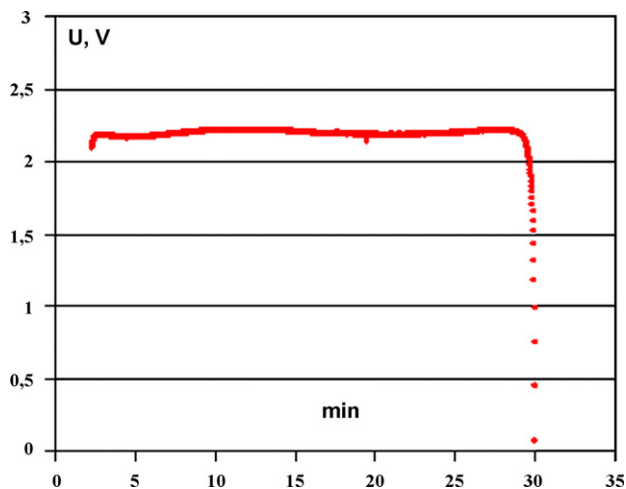


Fig. 11. Change in total voltage of the battery consisting of two two-cell stacks during joint WAHMG + FC tests.

on the total output of hydrogen in WAHMG and hydrogen losses due to purges of the gas system.

5. Conclusions

In the present article we described the prototype of the compact external 2W PS based on “free-breathing” FCs and the water–aluminum hydrogen micro-generator.

During experiments with FCs, a number of aspects of their operation under various external conditions, these are in the NCUV, NCCG, and FCCG modes, were studied at various rates of cathode gap purging. By comparison of the NCUV and NCCG modes it has been established that FC characteristics are better in the NCCG mode (operating conditions of two-cell FC stacks in PS body closely approach NCCG mode conditions) than in the NCUV mode. This result confirms possibility of free-breathing FC stack accommodation in the compact charger case. It was determined in consideration of the FC operation in the FCCG mode at various speeds of FC cathode gap purging that there is an optimum purging speed at which the FC has maximum characteristics. In turn it shows the need to use a micro-fan in PS.

In process of joint WAHMG + FC testing, the value of electrical energy produced per gram of Al in the micro-PS was determined, and the behavior of basic functional system parameters during operation of the charger model was studied as well.

Acknowledgement

The authors acknowledge the National Innovation Company “New Energy Projects” for financial support.

References

- [1] A. Kundu, J.H. Jang, J.H. Gil, C.R. Jung, H.R. Lee, S.-H. Kim, B. Ku, Y.S. Oh, J. Power Sources 170 (2007) 67–78.
- [2] J.-H. Wee, J. Power Sources 11 (2007) 1720–1738.
- [3] C. Stone, E. Consultants, Fuel Cells Bull. 10 (2007) 12–15.
- [4] V.A. Legasov, V.K. Kotelnikov, B.K. Popov, Atomic and Hydrogen Power Engineering and Technology, Atomizdat, Moscow, 1978, issue 1, pp. 11–36.
- [5] N.S. Lidorenko, G.F. Muchik, Electrochemical Generators, Energoizdat, Moscow, 1982.
- [6] L. Soler, J. Macanas, M. Munoz, J. Casado, J. Power Sources 169 (2007) 144–149.
- [7] A.Z. Zhuk, A.E. Sheindlin, B.V. Kleymentov, E.I. Shkolnikov, M.Y. Lopatin, J. Power Sources 157 (2006) 921–926.
- [8] R.G. Sarmurzina, A.A. Presnjakov, D.V. Sokolsky, N.N. Mofa, R.K. Aubakirova, G.G. Kurapov, J. Phys. Chem. 58 (4) (1984) 975–976.
- [9] C.R. Jang, A. Kundu, B. Ku, J.H. Gil, H.R. Lee, J.H. Jang, J. Power Sources 175 (2008) 490–494.
- [10] O.V. Kravchenko, K.N. Semenenko, B.M. Bulychev, K.B. Kalmykov, J. Alloys Compd. 397 (2005) 58–62.
- [11] B.S. Richardson, J.F. Birdwell, F.G. Pin, J.F. Jansen, R.F. Lind, J. Power Sources 145 (2005) 21–29.
- [12] J.-H. Wee, K.-Y. Lee, S.H. Kim, Fuel Process. Technol. 9 (2006) 811–819.
- [13] N. Mohajeri, A.T. Raissi, O. Adebijoyi, J. Power Sources 167 (2007) 482–485.
- [14] V.I. Simagina, P.A. Storozhenko, O.A. Komova, O.V. Netskina, J. Alternative Power Ecol. 7 (2006) 29.
- [15] M. Chandra, Q. Xu, J. Power Sources 156 (2006) 190–194.
- [16] X.-B. Zhang, S. Han, J.-M. Yan, M. Chandra, H. Shioyama, K. Yasuda, N. Kiriya, T. Kobayashi, Q. Xu, J. Power Sources 168 (2007) 167–171.
- [17] U.B. Demirci, J. Power Sources 172 (2007) 676–687.
- [18] A.S. Iljukhin, S.A. Tarasova, S.A. Yanushko, I.V. Yanilkin, E.I. Shkolnikov, Physical problems of hydrogen power engineering, The program and theses of reports, 2007, pp. 48–50.
- [19] S.A. Tarasova, S.A. Yanushko, A.V. Parmuzina, E.I. Shkolnikov, Physical problems of hydrogen power, Program and theses of reports, 2007, pp. 61–64.
- [20] M.S. Vlaskin, A.S. Iljukhin, I.V. Yanilkin, E.I. Shkolnikov, Physical problems of hydrogen power engineering, Program and theses of reports, 2007, pp. 137–140.
- [21] <http://www.gefc.com>.
- [22] K.R. Cooper, V. Ramani, J.M. Fenton, H.R. Kunz, Experimental Methods and Data Analyses for Polymer Electrolyte Fuel Cells, Scribner Associates Inc., NC, 2005, pp. 122.